

# Changes in Frequency of Electromagnetic Radiation from Loaded Coal Rock

Dazhao Song<sup>1,2</sup> · Enyuan Wang<sup>1,3</sup> · Xiaoyan Song<sup>4</sup> ·  
Peijian Jin<sup>5</sup> · Liming Qiu<sup>1</sup>

Received: 16 April 2014 / Accepted: 14 March 2015 / Published online: 11 April 2015  
© Springer-Verlag Wien 2015

**Abstract** To understand the relationship between the frequency of electromagnetic radiation (EMR) emitted from loaded coal rock and the micro-crack structures inside it, and assess the stress state and the stability of coal rock by analyzing frequency changes in characteristics of its emitted EMR, we first experimentally studied the changes in time sequence and the frequency spectrum characteristics of EMR during uniaxial compression, then theoretically derived the relationship between the principal frequency of EMR signals and the mechanical parameters of coal crack and analyzed the major factors causing the changes in the principal frequency, and lastly verified the results at Nuodong Coal Mine, Guizhou Province, China. The experimental results showed that (1) EMR intensity increased with the applied stress on loaded coal rock during its deformation and failure and could qualitatively reflect the coal's stress status; (2) with the applied stress increasing, the principal frequency gradually increased from near zero to about 60 kHz and then dropped to less than

20 kHz. During this period, coal rock first stepped into the linearly and elastically deformed stage and then ruptured around the peak load. Theoretical analysis showed that there was a negative correlation between the principle frequency and the size of internal cracks. Field detection showed that a lower principle frequency was generated from coal rock applied by a greater load, while a higher principal frequency was generated from coal rocks suffering a weaker load.

**Keywords** Coal rock · Electromagnetic radiation · Frequency spectrum analysis · Crack propagation · Stress assessment

## List of Symbols

$\omega$	Angular frequency
$b$	Crack width
$V_R$	Rayleigh wave speed
$K_I$	Stress strength factor of Type I cracks
$\sigma_s$	Yield stress
$E$	Elastic modulus
$\mu$	Poisson's ratio
$\sigma$	Applied stress
$a$	Half length of initial crack
$V_s$	Speed of the transverse wave

✉ Enyuan Wang  
weytop@cumt.edu.cn

<sup>1</sup> School of Safety Engineering, China University of Mining and Technology, Xuzhou 221116, China

<sup>2</sup> Postdoctoral Research Station, Yongcheng Coal and Electricity Holding Group Co. Ltd., Yongcheng 476600, China

<sup>3</sup> Key Laboratory of Gas and Fire Control for Coal Mines, Xuzhou 221008, China

<sup>4</sup> College of Applied Science and Technology, China University of Mining and Technology, Xuzhou 221008, China

<sup>5</sup> School of Municipal and Environmental Engineering, Jilin Jianzhu University, Jilin 130118, China

## 1 Introduction

Modeling (O'Keefe et al. 1995; Mognaschi 2002; Rabinovitch et al. 2007), laboratory investigations (Hadjicontis and Mavromatou 1994; Koktavy et al. 2004; Rabinovitch et al. 2001) and field measurements (Frid 2001; Frid and

Vozoff 2005; Lichtenberger 2006) have proven that coal rocks under deformation and failure process could produce electromagnetic radiation (EMR). In other words, the resultant EMR could accurately reflect the internal structure damages of coal rock materials and be used to effectively monitor and forecast dynamic disasters in coal mines. Based on this principle, an EMR monitoring and forewarning system with characteristics of directional, non-contacting, continuous detection, and forewarning has been developed by China University of Mining and Technology, and widely and successfully used to monitor and forecast rock bursts and coal as well as gas outbursts and to assess the stress status of coal rocks (Wang et al. 2011a, b).

The current EMR monitoring and forewarning techniques commonly utilize the time domain characteristics of EMR such as the radiation intensity and pulse number (Wang et al. 2011b), without giving enough attention to the frequency domain. However, some studies found that loaded coal rock emits EM signals of different frequency during its fracture and failure. For examples, Nitsan (1977) found that the maximum power of EMR lied in the frequency range of 1–2 MHz. Cress et al. (1987) observed that low-frequency EMR and visible light with frequencies of the order of magnitude of 1 kHz were emitted from fracturing non-piezoelectric basalt samples. Yamada et al. (1989) found that the frequency of EM signals emitted from fracturing granite was mostly above 0.5 MHz and their frequency spectrum was associated with the crack size and expanding rate. Qian et al. (1996) studied the characteristics of EMR with multiple frequency bands (VLF, MF, HF and VHF) during rock failure and found that the emitting time of EMR with different frequency bands were often not synchronized with ultra-low frequency signal and usually appeared first. Guo and Liu (1995) established an electric quadrupole model, calculated the frequency of the near electromagnetic field, and found that the frequency of the near electromagnetic field was related to the size of coal samples and the length of initial cracks and was about 50 kHz–1 MHz for granite samples with typical sizes and lengths of initial cracks. Liu et al. (1997) experimentally found that rock during its rupture could produce EM signals of high frequency (1–5 MHz), intermediate frequency (100 kHz–1 MHz), and low frequency (100 Hz–100 kHz).

The principal frequency (the frequency of the maximum amplitude in a frequency spectrum, generally consisting of a number of different and adjacent frequency signals) of EMR emitted during coal loading and failure varies. Based on the idea of EMR produced by atoms disturbed by rock fracturing and cracks propagating, Rabinovitch et al. (1998) first put forward a single pulse signal model. Based on their semi-empirical analysis and experimental studies, they found that the peak time of single EMR pulse was related to the rupture length of cracks, while its frequency

was related to the rupture width of cracks. Wang et al. (2003) found through laboratory studies that the EMR frequency spectrum of loaded coal rocks was from a few Hz to several MHz in the process of deformation and fracture and its principal frequency band changes with the applied load.

Coal rock contains a large number of defects with different scales. Its emitted EMR during loading could reflect the deformation and failure of coal rock at some extent. Thus, measuring EMR during its deformation and failure could help us understand the evolution of internal defects and cracks in the coal rock, analyze their stability, make corresponding pre-warning, and promote safety of coal mine production. However, previous researches were mainly focused on multi-frequency EMR to reveal the mechanisms of fracturing-induced EMR on the micro- and meso-scales and the relationship of the frequency of EMR signals to the size of single crack, while rarely on the in-depth studies on the macroscopic and statistical characteristics of EMR frequencies and their correlation with applied loading that determines the damage state of coal rock structure.

In this study, to establish a new method to early warn dynamic disasters of coal rock based on the changes in EMR frequency, we first conducted uniaxial compression experiments of coal rocks to study the changes in time sequence and the frequency spectrum features of EMR signals from coal rocks subjected to external loading during compression, then studied the characteristics of changes in the principal frequency of EMR signals and analyzed its main affecting factors, and last measured the frequency-varying characteristics of EMR signals from a large scale coal rock mass in the loading conditions at Nuodong Coal Mine, Guizhou Province, China.

## 2 Experiments

### 2.1 Experimental Devices

Figure 1 shows the EMR test system consisting of loading system, data acquisition system, and electromagnetic shielding system. The loading system is a YAW4306 servo-controlled mechanical equipment and has maximum load capacity of  $3.0 \times 10^3$  kN, force resolution of 1/300,000 with relative error rate of 1 %, and loading rate of 600–60,000 N/s with accuracy of  $\pm 1$  %. It has two control modes, the displacement mode and the force mode, and could be used for uniaxial compression, tension, cyclic loading, creep tests, etc. The data acquisition system is a PCI-2 AE system manufactured by Physical Acoustic Corporation and equipped with a board of 18-bit A/D conversion scheme, eight digital I/O, two complete high-

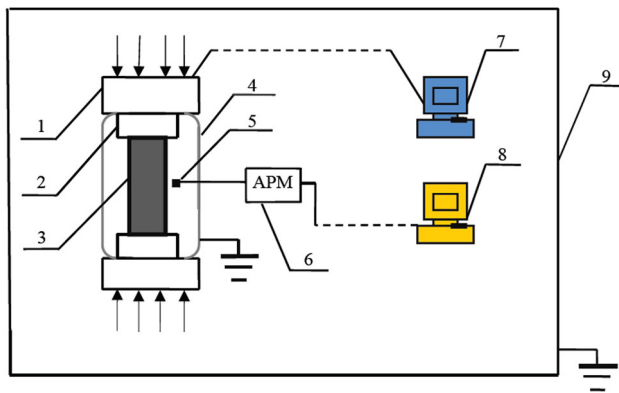


**Fig. 1** Schematic of experimental system

speed channels for real-time data acquisition, real-time feature extraction, waveform processing and transfer, and frequency response of 3 kHz–3 MHz at  $-3$  dB points. The electromagnetic shielding system is a GP6 electromagnetic shielding room with effectiveness of 14 kHz  $\geq 80$  dB, 100 kHz  $\geq 100$  dB, 300 kHz  $\geq 110$  dB and 50 MHz to 1 GHz  $\geq 110$  dB. In addition, to avoid the electromagnetic interference from electricity power, radio wave, and some electric equipments, etc., a double copper grid with size less than 0.2 mm was used to cover the coal samples. The coaxial shielded cable was used to connect the sensor and the data recorder.

## 2.2 Sample Preparation

Coal samples were extracted from No. 26 coal seam, Nuodong Coal Mine. The mine seam contained 0–3 layers of gangue and had average thickness of 2.81 m, gas content of  $14.3 \text{ W/m}^3 \text{ t}^{-1}$ , gas pressure of 0.88–0.94 MPa, permeability coefficient of 0.013145–0.017010, and firmness coefficient of 0.34–0.35. Its roof was argillaceous sandstone or mudstone, and its bottom was mudstone or carbonaceous mudstone. The sampling site was shown in Fig. 2.

The samples were prepared as standard cylindrical coal rock samples with diameter of 50 mm and length of 100 mm according to the regulation of the International Society for Rock Mechanics (ISRM) at the Strata Control Experimental Center of State Key Laboratory of Coal Resources and Safe Mining, China University of Mining and Technology. All samples were properly labeled with number, and put in an airtight glass container sealed with vaseline to keep their original states.

## 2.3 Experimental Program

We carried out a series of experiments with coal rock samples loaded under the uniaxial compression at the

loading rate of 0.01 mm/s using the displacement mode and simultaneously measured EM signals emitted from the samples.

## 2.4 Experimental Results and Analysis

### 2.4.1 Changes in Time Sequence of EM Signals from Loaded Coal Samples

Figure 3 shows the typical characteristics of EM signal from the coal samples during failure process due to uniaxial compression. From the initial loading to 150 s when the loading strength was about 10 % of the peak, EM signal was relatively stable with cumulative intensity in a second fluctuating around 40 mV. Between 150 and 300 s, EMR intensity rose nearly linearly with the loading strength increasing, i.e., EMR changes were consistent with that of the load value. At 297 s when the loading strength was about 59.3 % of the peak, the EMR intensity reached its peak. After that, it dropped to its low valley which lasted for about 50 s. When the loading strength was about 85 % of the peak, EMR intensity rose rapidly until the end of the loading.

Coal samples contain numerous pores and cracks and have relatively lower strength. Under loading, these pores and cracks will close, causing the deformation and micro-cracks of coal mass near the crack walls, which are sufficient to emit EMR. Because almost all micro-cracks are involved in this process, the produced EM signals are much more than that in the elastic deformation stage. As shown in Fig. 3, 150 s prior to loading, EM signal shows a non-obvious decreasing trend.

After full pore closure of coal samples, as shown at Point A in Fig. 3, with continuous loading, both the stress and EM signal curves show elastic characteristics, indicating that under a relatively smaller load, coal samples undergo stable elastic deformation and micro-cracking. Correspondingly, EM signal continuously increases at a relatively stable rate. The state lasts to the stress reaching about 60 % of its peak.

After Point B in Fig. 3, EM signal disappears about 50 s, possibly because of the relatively complete failure of small structural units with less strength during the pre-loading process, and insufficient failure of large structural unit, the so-called skeleton structure (Zweben and Rosen 1970). At this point, the applied stress and coal sample form a quasi-static equilibrium. In other words, the external energy applied on the sample is fully absorbed or stored as the elastic energy of the skeleton structure, which significantly reduces the micro-cracking of coal units, resulting in the decreased EM signal.

When the external stress continues to increase and reaches about 90 % of the peak, the above-mentioned equilibrium is broken. The skeleton strength is not enough

**Fig. 2** Schematic of sampling site

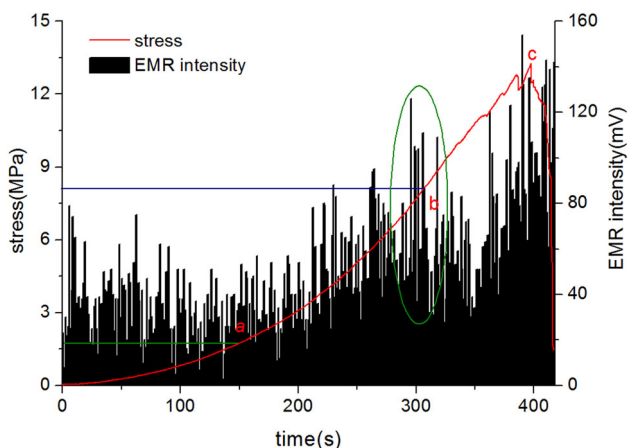
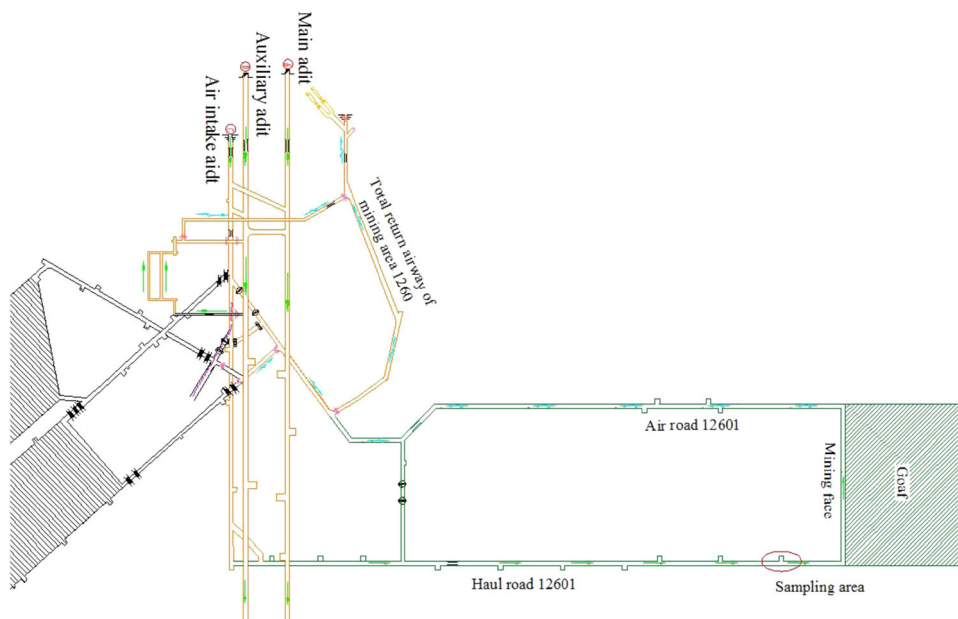


**Fig. 3** EMR intensity curve and stress–time curve during the uniaxial compression and failure of coal samples (EMR intensity in histogram is the accumulative value of various EM signal bands in a second)

to resist against the external stress, thus pores and cracks are destroyed within a very short time and macrocracks undergo fusion connection and combination, resulting in the complete failure of coal samples and emission of a large amount of EMR.

Overall, the EMR intensity is positively correlated with the external stress and can effectively reflect the internal stress status of coal samples.

**2.4.2 Frequency Changes in EMR from the Loaded Coal**

At the pore closure stage (Wang et al. 2003), as shown as the 0–a part before 10 %  $\sigma$  in Fig. 3, the frequency of emitted EM signals is in the range of 0–100 kHz. Its

principal frequency band changes in a trend of first increasing to up to 10 kHz and then decreasing to its previous level but with less intensity of about 10 dB (Fig. 4a, c), consistent with the previous report (Wang et al. 2003). With the external loading increasing (a, b part of Fig. 3), the coal sample enters the linear elastic deformation stage; the frequency of principal signal increases, reaching and maintaining at over 60 kHz when the applied load is about 50 %  $\sigma$ . Meanwhile, EM signal intensity evidently enhances in a broader frequency range, as shown in Fig. 4c–f. As the loading increases from 70 %  $\sigma$  to 100 %  $\sigma$ , the frequency of the principal signals gradually lowers, dropping to 20 kHz at the peak load. However, the intensity of EM signals remains at a high level, close to 20 dB, as shown in Fig. 4g, h. After the peak load, the main frequency of EM signals keeps below 20 kHz and power spectral intensity lowers slightly, as shown in Fig. 4i, j.

**2.4.3 Frequency Changes of EM Signals from Loaded Coal Samples**

**2.4.3.1 Factors Affecting EM Signal Frequency** The generation and expansion of internal micro-cracks of coal rocks subjected to loading can produce and emit EMR. Thus, it is important to investigate the relationship between the properties of microscopic cracks and EM signals and to understand the crack nucleation and evolution processes.

According to the wave theory (Bakshi and Bakshi 2009), the relationship of frequency  $\omega$  of a wave propagating at a speed  $V$  to its wavelength  $\lambda$  could be expressed as.

$$\omega = \frac{2\pi V}{\lambda} \tag{1}$$

Based on the formula, Rabinovitch et al. (1998) found that when a crack propagates or expands forward, the atom bond originally located at the end of the crack ruptures, leading to break and disturbance of non-equilibrium state of atoms around the atom bond. This atomic perturbation could induce coal emitting EMR. However, the atomic perturbation at both sides of a crack is restricted, i.e., the wavelength of atomic perturbation is limited by the width of the crack. Thus, the relationship between the frequency of EMR induced by crack propagation and the crack width is introduced as follows:

$$\omega = \frac{\pi V}{b} \tag{2}$$

where  $\omega$  is the angular frequency,  $b$  is the crack width, and  $2b$  is the wavelength of atomic perturbation. To verify the

formulas, Frid introduced the measured crack width and corresponding EMR frequency into this formula, and obtained the wave speed which was equal to the Rayleigh wave speed  $V_R$  (Frid et al. 2003), that is

$$\omega = \frac{\pi V_R}{b} \tag{3}$$

In Eq. (3),  $V_R$  can be calculated according to the physical mechanic parameters of coal rock. Thus, if the crack width of coal rock in its rupture process is given, the corresponding frequency of EM signals from the coal rocks can be found.

In the fracture mechanics theory, cracks are distinguished into three basic modes based on the deformation form of rock surface under the external stress: Mode I or the opened, Mode II or the slipped, and Mode III or the torn (Anderson 2005). For

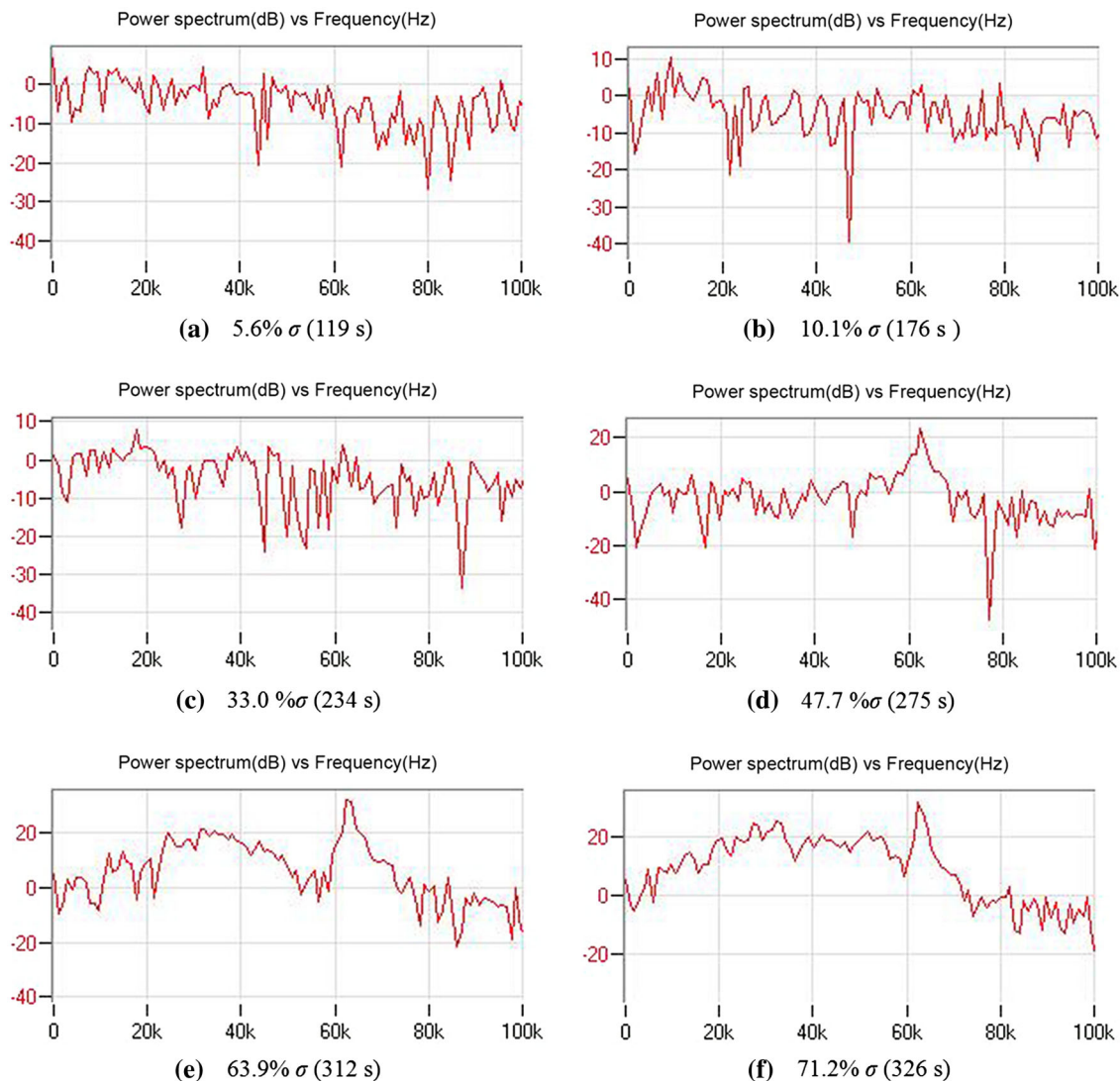


**Fig. 4** Variation in principal band of EMR in different stress levels from the coal sample loading process (a–h are before peak stress, while i, j are after peak stress)

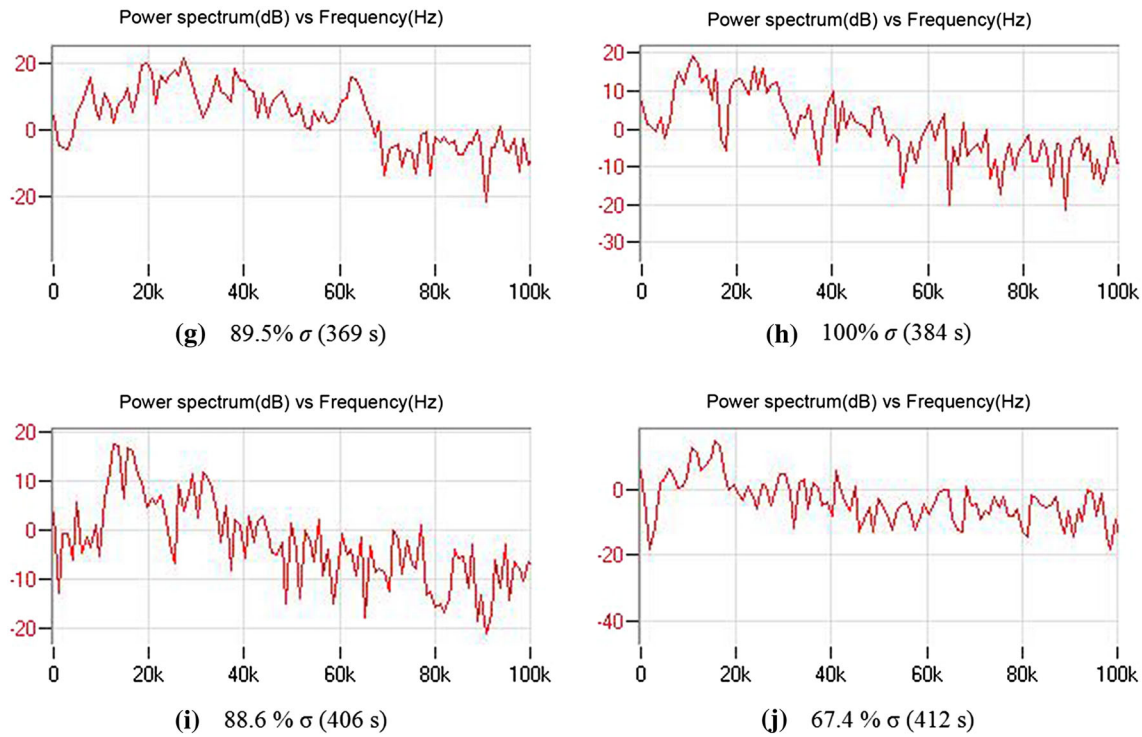


Fig. 4 continued

Mode I cracks, the cracking opening displacement (COD) of the original crack tip is  $\delta$  when it opens and expands from point  $O$  to point  $O'$ . In the condition of a small-scale yield, COD of Mode I cracks can be obtained from the following formulas (Reches and Lockner 1994; Naman 2012):

$$\delta = \begin{cases} \frac{4 K_I^2}{\pi \sigma_s E} & \text{(Planestress)} \\ \frac{2\sqrt{\sqrt{2}}(1-\mu^2)K_I^2}{\pi \sigma_s E} & \text{(Planestrain)} \end{cases} \quad (4)$$

where  $K_I$  is the stress strength factor of Mode I cracks,  $\sigma_s$  is the yield stress,  $E$  is the elastic modulus, and  $\mu$  is the Poisson's ratio. In general,  $\sigma$  is taken  $\leq 0.6 \sigma_s$ .

For a long through crack, rock fracture is considered as the problem of plane strain, its stress strength factor is

$$K_I = \sigma\sqrt{\pi a} \quad (5)$$

From Eqs. (5) and (4),

$$\delta = \frac{2\sqrt{\sqrt{2}}(1-\mu^2)(\sigma\sqrt{\pi a})^2}{\pi \sigma_s E} \quad (6)$$

where  $\sigma$  is the applied stress and  $a$  is the half length of the initial crack.

When  $\delta = \delta_c$ , we obtain the critical load at the beginning of crack expansion:

$$\sigma_0 = \sqrt{\frac{\delta_c \sigma_s \cdot E}{2\sqrt{\sqrt{2}} \cdot (1-\mu^2) \cdot a}} \quad (7)$$

From Eqs. (7) and (5),

$$K_I = \sqrt{\frac{\pi \delta_c \sigma_s \cdot E}{2\sqrt{\sqrt{2}} \cdot (1-\mu^2)}} \quad (8)$$

As shown in Fig. 5, the distance the crack tip moves forward due to its expansion is

$$r = \begin{cases} \frac{1}{2\pi} \left(\frac{K_I}{\sigma_s}\right)^2 & \text{(Plane stress)} \\ \frac{1}{4\sqrt{2}\pi} \left(\frac{K_I}{\sigma_s}\right)^2 & \text{(Plane strain)} \end{cases} \quad (9)$$

Substituting Eq. (8) for the second formulas of Eq. (9) finds the displacement of the crack tip at its expansion:

$$r_y = \frac{\delta_c \cdot E}{8\sqrt{\sqrt{2}}\sigma_s(1-\mu^2)} \quad (10)$$

When the crack expands any length  $r$  along its tip ( $r$  may be larger or smaller than  $r_y$ ),  $r$  varies depending on the tip expansion process. At this point, suppose the crack width is  $b$ , thus the simplified formula is as  $BB'$  shown in Fig. 5. Based on the geometrical relation,

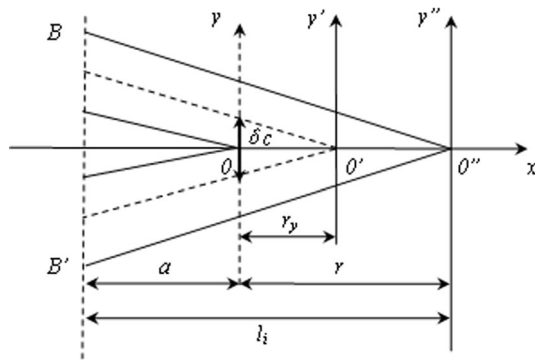


Fig. 5 Schematic of crack expansion in coal rock

$$\frac{b}{\delta_c} = \frac{a + r}{r_y} \tag{11}$$

From (10) and (11), we can find

$$b = 8\sqrt{\sqrt{8}(a + r)(1 - \mu^2)} \frac{\sigma_s}{E} \tag{12}$$

Again substituting (12) for (3), the frequency of EM signal is

$$f = \frac{V_R}{2b} = V_R \frac{E}{16\sqrt{\sqrt{8}(a + r)(1 - \mu^2)}\sigma_s} \tag{13}$$

According to the elastic mechanics (Timoshenko and Gere 2009), Rayleigh wave speed is

$$V_R = \frac{0.87 + 1.12\mu}{1 + \mu} V_s \tag{14}$$

where  $V_s$  is the speed of the transverse wave, i.e.,

$$V_s = \sqrt{\frac{E}{2(1 + \mu)\rho}} \tag{15}$$

Comprehensive consideration of (13)–(15) leads to the relationship between the frequency of EM signals produced by crack expansion and the physical parameters of coal rocks as

$$f = \frac{1}{32\sqrt{\sqrt{2}(a + r)}} \frac{(0.87 + 1.12\mu)E^{\frac{3}{2}}}{(1 - \mu)(1 + \mu)^{\frac{5}{2}}\sigma_s\rho^{\frac{1}{2}}} \tag{16}$$

To facilitate the study, the sum of the initial crack length and the extended length is defined as the crack length, i.e.,  $l_i = a + r$ . Because most of the coal rock materials are brittle ones, the yield strength of a coal rock is close to its compressive strength, i.e.,  $\sigma_s = \sigma_c$ . Thus, the frequency of EM signals becomes:

$$f = \frac{1}{32\sqrt{\sqrt{2}l_i}} \frac{(0.87 + 1.12\mu)E^{\frac{3}{2}}}{(1 - \mu)(1 + \mu)^{\frac{5}{2}}\sigma_c\rho^{\frac{1}{2}}}, (l_i > a) \tag{17}$$

From Eq. (17), the frequency of EM signals and the crack length have an inversely proportional relationship, assuming its density, elastic modulus, Poisson’s ratio and strength are unchanged.

Because the above mechanical parameters are invariant for coal samples used in the laboratory experiments and approximately unchanged for coal rocks from the same coal seam in the field tests, it is reasonable that the changes in the frequency of the same coal sample are caused by the changes of internal crack size through equilibrium and expansion. Therefore, our laboratory and field experimental results are discussed from the point of view of the crack size.

**2.4.3.2 Analysis of Frequency Changes Based on Crack Expansion** As a typical heterogeneous anisotropic material, coal rocks contain a large quantity of internal cracks, pores, and other native defects of low strength and various sizes. At the pore closure stage of loading, these defects undergo damage at lower loading stress and radiate EM signals, which have apparently random and varied frequency and show no obvious principal frequency band on the oscillogram. Meanwhile, the destabilizing and expanding of small-scale cracks and defects lead to emitting EM signals of low intensity, showing the power spectrum curve fluctuates around the base line, as shown in Fig. 4a, b.

With the load continuous to increase, coal is gradually compacted and enters its linear elastic stage. When the energy of a certain region inside the coal reaches or exceeds its carrying capacity, rupture happens in this area producing micro-cracks. These micro-cracks will stop fracturing, accelerate expansion, converge and coalesce with their neighboring micro-cracks depending on the energy distribution in the region. During this stage, a large number of micro-cracks with smaller sizes start extension, resulting in a bigger principal frequency band of EMR. With the loading enhancing, the intensity of EM signals increases, showing broader frequency band of EM signals with higher power spectral density, as shown in Fig. 4c–f.

During the mid- to late loading stages, the internal structure units of coal undergo self-organization, producing a large number of mesoscopic cracks by converge and coalesce, and gradually form macroscopic cracks with greater size. Thus, the internal structure of coal undergoes “dimension reduction” or “entropy reduction”. In other words, the cracks’ distribution and expansion process is characterized by orderliness (Qin 2000). In this process, the EM signals gradually change from high frequency to low frequency till the failure occurs after peak load. At this stage, the principle frequency band remains around 20 kHz, but has more signals compared with the pore closure stage of loading, as shown in Fig. 4g–j.

### 3 Field Experiments

#### 3.1 Field Overview and Instruments

##### 3.1.1 Field Overview

The field site was the Mining face No. 11801 of Nuodong Coal Mine, Guizhou Xing'an Coal Ltd., Guizhou Province, China. It has a inclination length of 124 m, strike length of 320 m, and average mining height of 2.2 m. Its immediate roof plate is silty mudstone and siltstone and its immediate bottom is mudstone and silty mudstone. The average dip angle of its coal strata is  $4^\circ$ . Affected by a microstructure, some sections of coal seams appear somewhat undulant. The roof plates developed near microstructures or cracks are prone to fragmentation and caving. The coal bed structure has only 0–1 layer of gangue with average thickness of 0.2 m and consists mainly of mudstone and locally silty mudstone. Currently, the face has mined about 80 m without apparent dynamic manifestation.

##### 3.1.2 Experimental Instruments

The instrument used for the field experiments was a portable YDD16 acoustic–electric monitor for coal rock dynamic disasters. The device has multi-channels, multi-signals as well as non-contact directional monitoring features, and consists of main monitoring system, wide band EMR directional antenna, ultra-low frequency EM induction antenna, acoustic emission probe, microseismic probe, charger, communication cables and data processing system, as shown in Fig. 6. The device can be used to measure acoustic and electromagnetic radiations emitted from the loaded coal rocks during deformation and failure for the prediction of coal rock dynamic disasters.

The monitor has the following main technical parameters: (1) ferrite antenna, (2) effective monitoring direction of  $60^\circ$ ; (3) effective monitoring range of 7–22 m, as shown in Fig. 7; (4) band width of received signals of 1–400 kHz and dynamic gain of 30 dBu; (5) instrument sensitivity of 1.61, 0.67 and 0.33 mV/m at preamplifier working at 46, 54, and 60 dB, respectively; and (6) instrument sampling frequency of 1–5 MHz. Further, the threshold of acquired signals was set at 50 mV, i.e., only signals equal to or larger than 50 mV were recorded.

#### 3.2 Measurement Method

According to its subjected stress status, the coal mass in front of the mining face can be generally divided into three zones: the relaxation zone, the stress concentration zone, and the original stress zone (Gale and Blackwood 1987), as



Fig. 6 YDD16 EMR monitor

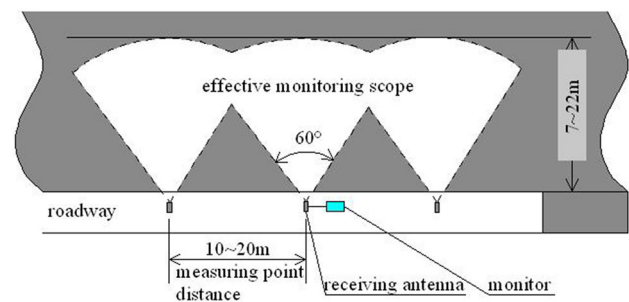


Fig. 7 Schematic of YDD16 monitor while working and its effective monitoring scope

shown in Fig. 8. A study has showed that the mining-affected zone within the working face could extend as far as tens of meters, sometimes even over 100 m (Yang et al. 2011).

A total of 11 testing points with interval of 10 m in the field experiments were selected beginning from the wall of the working face and covering a total length of 100 m in front of the working face, as shown in Fig. 9. YDD16 monitors were installed at each testing point with antenna oriented to the coal wall and fixed at the position of 1 m to the floor and 0.5 m from the face wall. EM signals at each testing point were monitored for 2 min. During the measurement, high-power electrical equipments were temporarily shut down to avoid signal interference with data acquisition.

During the field testing, the average EM signal intensity within 2 min at each measuring point was used to assess



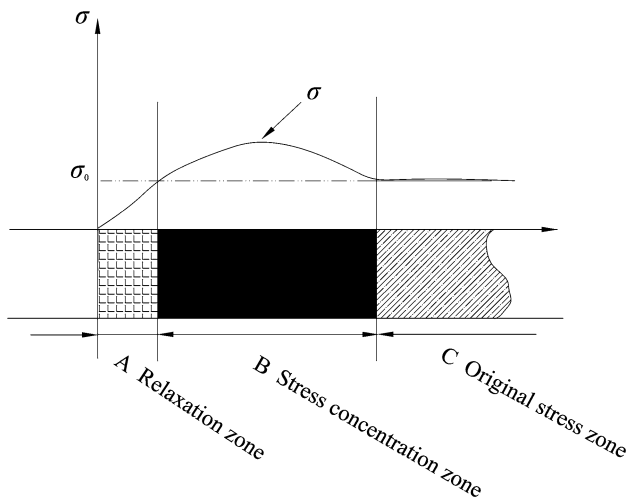


**Fig. 8** Schematic of stress distribution zones before coal mining face

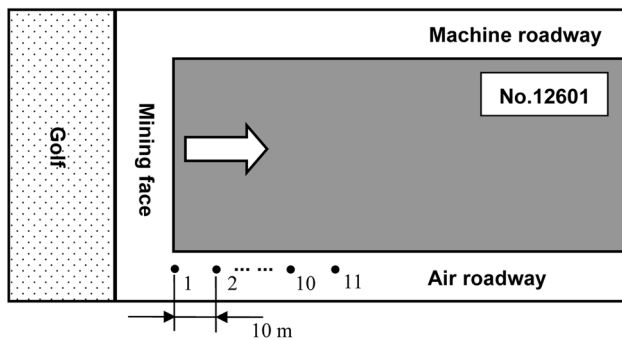


**Fig. 9** Schematic of measuring points distribution on coal mining field

the stress state at the testing point and analyze the effective EM signals acquired at each testing point.

### 3.3 Experimental Results and Analysis

Figure 10 shows the intensity of EM signals at all measuring points. According to Wang et al. (2011b), EMR measuring method can be applied to determine the stress distribution of roadway or face, high stress areas and active stress area and to reveal the surrounding rock stress distribution of the entire monitoring region. It is clearly seen from Fig. 10 that the region 30–40 m from the Face 11801 has higher EM signal intensity and is considered as the stress relief zone and stress concentration zone, outside of which is the original stress zone.

Figure 11 shows the typical power spectrum density curves of EM signals obtained by Fourier transformation using MATLAB software. It is obvious that in the range of 30 m in front of the mining face (i.e., the stress relaxation zone and the stress concentration zone), the principal frequency of EM signals is about  $0.5 \times 10^5$  Hz. With the

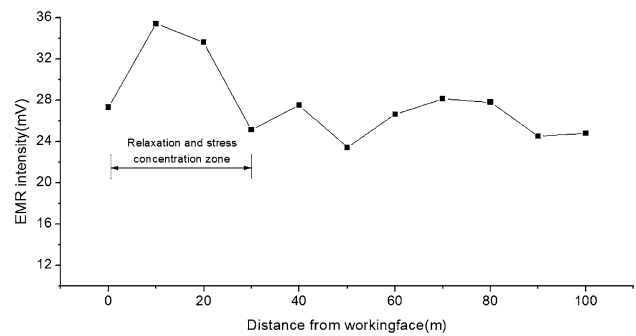


**Fig. 10** Distribution of EMR intensity measured in the front of Face 11801

increase of distance away from the face, the principal frequency gradually moves to the higher-frequency end. At the position of 40 m, the signals are radiated within three frequency bands of  $0-0.5 \times 10^5$ ,  $2 \times 10^5-2.5 \times 10^5$  and  $3 \times 10^5-3.5 \times 10^5$  Hz, respectively. Beyond 50 m away, the signals have frequency bands within  $3 \times 10^5-3.5 \times 10^5$  Hz. However, the intensity gradually weakens.

The EM signals shown in Fig. 11b–d were acquired from the stress concentration zone, in which the stronger external load strength resulted in the production of a large number of internal macrocracks. Instability and expanding of these cracks lead to emission of a large amount of low-frequency EM signals. However, coals at this stage contain a large number of internal micro-cracks, which could emit higher-frequency EM signals (Fig. 4h). Meanwhile, the principal frequency band of EM signals produced from the stress relief zone shown in Fig. 11a was also low, possibly because the stress of coals in this zone had been released. However, because of no confining pressure in both face wall and roadway directions, the coal subjected to smaller load would gradually swell and deform. In addition, coal in this region were more prone to external disturbances; thus, those macrocracks formed previously would still slowly expand and produce large amount of low-frequency signals, corresponding to the post-peak stage in Fig. 4i, j.

Away from the face wall, the external load applied on coal gradually decreased till close to the original stress. The typical frequency spectrum shows that the principal frequency of EM signals has a trend of moving towards the high-frequency end with external load decreasing. While, in the initial stress zone, the main frequency signal further weakened and became obvious, corresponding to the early loading stage.

The above comparative analysis shows that the field experimental results are in a rough agreement with the laboratory results. The main frequency of EM signals from loaded coal is in or moves toward the low-frequency bands, indicating that under greater external loading, internal macrocracks are formed and extended. Therefore, the

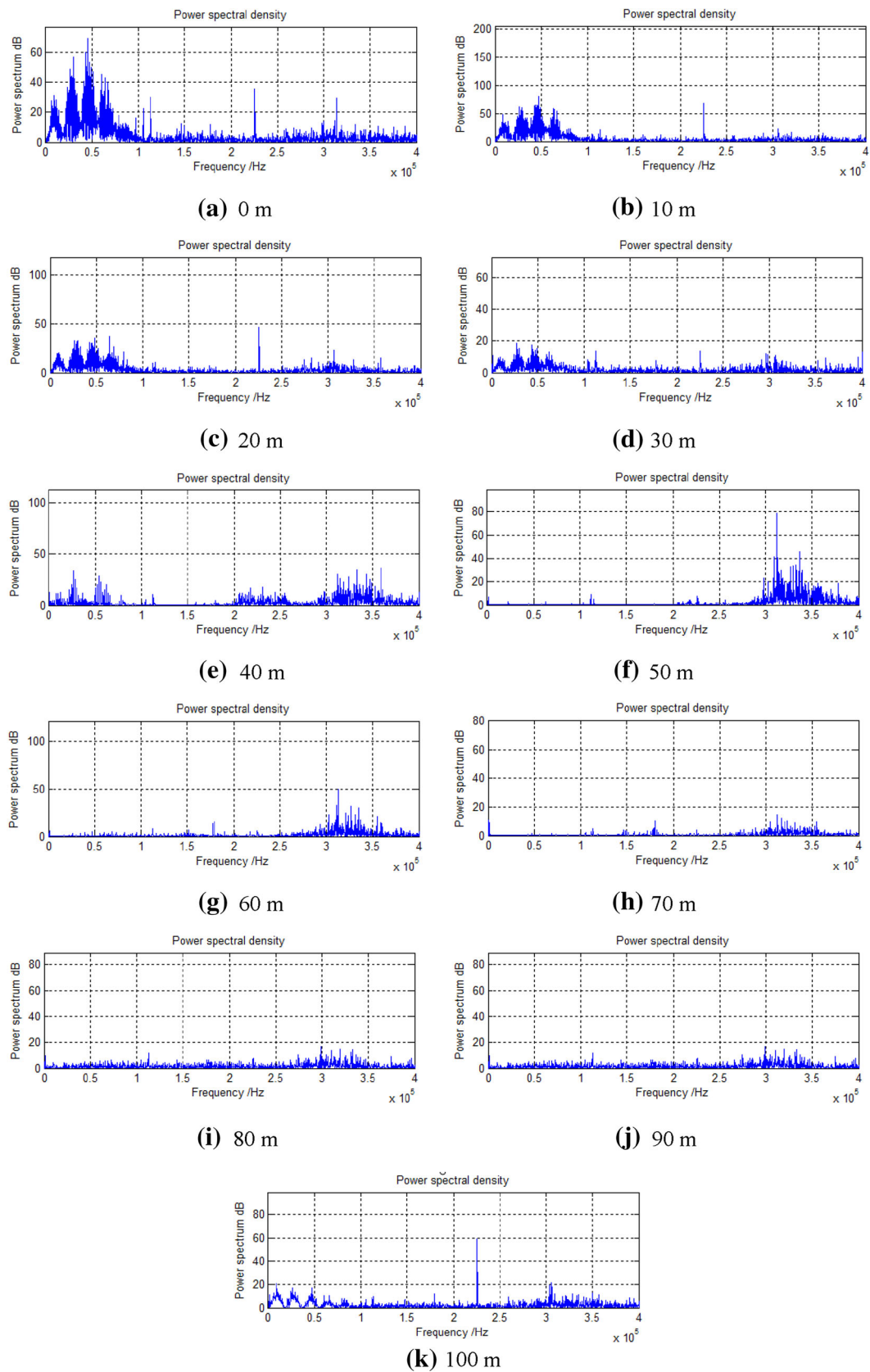


**Fig. 11** Power spectrum density of EMR signal measured at all the testing points

**Table 1** EM signal frequencies calculated from physical parameters of samples

Sample	Density $\rho$ (g/cm <sup>3</sup> )	Elastic modulus $E$ (GPa)	Poisson ratio ( $\mu$ )	Compressive strength $\sigma_c$ (MPa)	Lower limit $f_0$ (kHz)	Upper limit $f$ (MHz)
Sandstone	2.61	20	0.2	60	42	70.07
Coal	1.39	1.4	0.25	15	4.32	0.57

distribution and state of stress in coal rocks can be determined by the characteristics of frequency changes of measured EM signals. In practice, this frequency change can also be used to decide the stability of coal in combination with other boundary conditions such as whether coal rocks are in a tectonic zone, or whether the gas concentration is abnormal.

#### 4 Discussions

Assuming that instability and failure of coal rock samples are caused by cracks' independent expansion, according to Eq. (12), the frequency range of EMR signals from coal rock during its deformation and failure can be theoretically calculated. Since Eq. (12) is derived based on the assumption that coal rock is an infinity plate containing a large amount of internal cracks on the micrometers scale; this formula is suitable to coal rock with size larger than 1 m. Xu et al. (1986) considered two extreme conditions, one is that the minimum length of the crack is  $l_0$ , the other is that it runs completely through the length of the sample (the half length of the sample is  $l$ ), and concluded that the width and length of sandstone samples measured under microscope were 1–5  $\mu\text{m}$  and 20–200  $\mu\text{m}$ , respectively. Considering that the homogeneity of coal rock is far less than that of sandstone, we let  $l_0 = 1000 \mu\text{m}$ . In addition, considering that Eq. (12) is more suitable for samples with large size and the reality of underground mining, we let  $l = 50 \text{ cm}$ . Experimental observations (Qian et al. 1996) of rock samples with different lengths (28–36 cm) showed that the range of changes in the frequency of EMR signals produced by coal rock fracturing was very wide, covering 20 Hz–10 kHz in VLF, 530 kHz, 650 kHz, 1.65 MHz and 2.3 MHz in MF, 5 and 16 MHz in HF, and 95 MHz in VHF.

The physical parameters of coal and sandstone were first determined based on the previous researches (Han 1996; Meng et al. 2002; and Sivakugan et al. 2013) and the mechanical parameters of Nuodong Coal Mine. The range of EMR frequencies was then calculated through Eq. (12), as listed in Table 1. From the table, it is obvious that the frequency range of EM signals produced in the process of coal rock deformation and failure is very wide, covering from several kHz to several hundred kHz. The calculated

results are very close to the frequency bands measured experimentally by Qian et al. (1996).

Equation (12) is derived based on the independent expansion of a single crack in coal rock; thus, the calculated result is corresponding to EMR frequency range. The characteristics of frequency change in EMR signals as discussed herein (Fig. 3) are statistical ones. Figure 4 shows the typical frequency spectra corresponding to different stages. However, the production of different spectra is closely related to the external load at that time. For example, only in the intermediate stage of loading, the waveforms with an evident principal frequency at a relative high-frequency end can be produced in large quantities as shown in Fig. 4d–f, while at the early stage of loading, no such waveforms can be obtained. Thus, through statistical analysis of the features of EMR signal frequency change in the process of loading, one can determine the state of coal rock subjected to stress from the rupture point of view, and further assess its stability.

Equation 12 reveals the natural relationship between the frequency of EMR signals from loaded coal rock and their physical parameters. The frequency is closely related to the extent of crack fracturing, but independent of the bearings of the testing point relative to the field source (Guo and Liu 1995). Therefore, the frequency of EMR signals is one of the important parameters reflecting the characteristics of EMR signals from coal rock.

#### 5 Conclusions

1. EMR is resulted from deformation and failure of coal rock. Its intensity is positively proportional to the applied stress and could effectively reflect the state of coal subjected to stress.
2. With the applied stress gradually increasing, the principal frequency of EMR signals increases gradually from no obvious manifestation to about 60 kHz as coal stepped into the stage of linear elastic deformation, and then decreases to less than 20 kHz around the peak load during coal rupture.
3. The signal frequency is closely related to the physical and mechanical parameters of coal rock such as the crack size, material density, elastic modulus, Poisson's

ratio, and material strength, and changes with the size of internal cracks.

4. The field detection at Nuodong Coal Mine showed that the frequency band with a lower principle frequency was emitted when the coal was subjected to a greater external load, while the principal frequency became higher as the load became weaker. This phenomenon can be used to determine the stability of coal rock at coal mines combined with other field boundary conditions, such as whether the coal rock is in the structural zone, and whether the gas concentration is abnormal, etc.

**Acknowledgments** This work is supported by the Youth Science Foundation of the National Natural Science Foundation of China (51104156), the China Postdoctoral Science Foundation (2014T70678) and the Priority Academic Program Development of Jiangsu Higher Education Institutions.

## References

- Anderson TL (2005) *Fracture mechanics: fundamentals and applications*. CRC Press, Boca Raton
- Bakshi UA, Bakshi AV (2009) *Electromagnetic field theory*. Technical Publications
- Cress GO, Brady BT, Rowell GA (1987) Sources of electromagnetic radiation from fracture of rock samples in laboratory. *Geophys Res Lett* 14:331–334
- Frid V (2001) Calculation of electromagnetic radiation criterion for rock burst hazard forecast in coal mines. *Pure appl Geophys* 158:931–944
- Frid V, Vozoff K (2005) Electromagnetic radiation induced by mining rock failure. *Int J Coal Geol* 64:57–65
- Frid V, Rabinovitch A, Bahat D (1999) Electromagnetic radiation associated with induced triaxial fracture in granite. *Philos Mag Lett* 79:79–86
- Frid V, Rabinovitch A, Bahat D (2003) Fracture induced electromagnetic radiation. *J Phys D Appl Phys* 36:1620–1628
- Gale WJ, Blackwood RL (1987) Stress distributions and rock failure around coal mine roadways. *Int J Rock Mech Min Sci* 24:165–173
- Guo Z, Liu B (1995) Frequency properties of electromagnetic emission associated with microscopic cracking in rocks. *Acta Geophysica Sinica* 38:221–226
- Hadjicontis V, Mavromatou C (1994) Transient electric signals prior to rock failure under uniaxial stress. *Geophys Res Lett* 21:1687–1690
- Han D (1996) *China Coal Petrography*. China University of Mining and Technology Press, Xuzhou
- Koktavay P, Pavelka J, Sikula J (2004) Characterization of acoustic and electromagnetic emission sources. *Meas Sci Technol* 15:973–977
- Lichtenberger M (2006) Underground measurements of electromagnetic radiation related to stress-induced fractures in the Odenwald Mountains (Germany). *Pure appl Geophys* 163:1661–1677
- Liu Y, Liu Y, Wang Y, Jin A, Fu J, Cao J (1997) Factors and mechanisms of electromagnetic radiation when rock cracking. *Acta Seismol Sin* 19:418–425
- Meng Z, Peng S, Fu J (2002) Study on control factors of rock mechanics properties of coal-bearing formation. *Chin J Rock Mech Eng* 21:102–106
- Mognaschi ER (2002) On the possible origin, propagation and detectability of electromagnetic precursors of earthquakes. *Atti Ticinensi di Scienze della Terra* 43:111–118
- Naman R (2012) *Fracture mechanics and crack growth*. Wiley-Iste, New York
- Nitsan U (1977) Electromagnetic emission accompanying fracture of quartz-bearing rocks[J]. *Geophys Res Lett* 4:333–336
- O’Keefe SG, Thiel SV (1995) A mechanism for the production of electromagnetic radiation during fracture of brittle materials. *Phys Earth Planet Inter* 1–2:127–135
- Qian S, Ren K, Lv Z (1996) Experimental study on electromagnetic emission(VLF, MF, HF and VHF) characteristics during rock cracking processes. *Acta Seismol Sin* 18:346–351
- Qin S (2000) Primary discussion on formation mechanism of dissipative structure in instability. *Chin J Rock Mech Eng* 19:265–269
- Rabinovitch A, Frid V, Bahat D (1998) Parametrization of electromagnetic radiation pulses obtained by triaxial fracture of granite sample. *Philos Mag Lett* 77:289–293
- Rabinovitch A, Frid V, Bahat D (2001) Gutenberg-Richter-type relation for laboratory fracture induced electromagnetic radiation. *Phys Rev* 65:011401–011404
- Rabinovitch A, Frid V, Bahat D (2007) Surface oscillations—a possible source of fracture induced electromagnetic radiation. *Tectonophysics* 431:15–21
- Reches Z, Lockner DA (1994) Nucleation and growth of faults in brittle rocks. *J Geophys Res* 99:18159–18173
- Sivakugan N, Shukla SK, Braja MD (2013) *Rock Mechanics*. Taylor and Francis, Boca Raton
- Timoshenko SP, Gere JM (2009) *Theory of elastic stability*. Dover Publications, New York
- Wang E, He X, Liu Z, Zhou S (2003) Frequency spectrum characteristics of electromagnetic emission of loaded coal. *J China Univ Min Technol* 32:487–490
- Wang E, He X, Liu X, Li Z, Wang C, Xiao D (2011a) A non-contact mine pressure evaluation method by electromagnetic radiation. *J Appl Geophys* 75:338–344
- Wang E, He X, Wei J, Nie B, Song D (2011b) Electromagnetic emission graded warning model and its applications against coal rock dynamic collapses. *Int J Rock Mech Min Sci* 48:556–564
- Xu J, Li H, Xian X, Yin G (1986) Experimental study of the whole development process of micro-fracture in sandstone under uniaxial stress state. *Mechan Eng* 4:16–21
- Yamada I, Masuda K, Mizutani H (1989) Electromagnetic and acoustic emission associated with rock fracture[J]. *Phys Earth Planet Inter* 57:157–168
- Yang W, Lin B, Qu Y, Li Z, Zhai, Cheng, Jia L, Zhao W (2011) Stress evolution with time and space during mining of a coal seam. *Int J Rock Mech Mining Sci* 48:1145–1152
- Zweben C, Rosen BW (1970) A statistical theory of material strength with application to composite materials. *J Mech Phys Solids* 18:189–206